

¹ KPM.jl: A Julia Package for Kernel Polynomial Method in Condensed Matter Physics

³ **Ang-Kun Wu**  ^{1,3}, **Yixing Fu**  ¹, **Justin H. Wilson**  ^{4,5}, and **J. H. Pixley**  ^{1,2¶}

⁵ 1 Department of Physics and Astronomy, Center for Materials Theory, Rutgers University, Piscataway,
⁶ New Jersey 08854, USA 2 Center for Computational Quantum Physics, Flatiron Institute, 162 5th
⁷ Avenue, New York, New York 10010, USA 3 Department of Physics and Astronomy, University of
⁸ Tennessee, Knoxville, Knoxville, Tennessee, 37996, USA 4 Department of Physics and Astronomy,
⁹ Louisiana State University, Baton Rouge, LA 70803, USA 5 Center for Computation and Technology,
¹⁰ Louisiana State University, Baton Rouge, LA 70803, USA ¶ Corresponding author

DOI: [10.xxxxxx/draft](https://doi.org/10.xxxxxx/draft)

Software

- [Review](#) 
- [Repository](#) 
- [Archive](#) 

Editor: [Open Journals](#) 

Reviewers:

- [@openjournals](#)

Submitted: 01 January 1970

Published: unpublished

License

Authors of papers retain copyright
and release the work under a
Creative Commons Attribution 4.0
International License ([CC BY 4.0](#))

¹¹ Summary

¹² The Kernel Polynomial Method (KPM) is a numerical technique for approximating spectral
¹³ densities and response functions of large Hermitian operators without performing full
¹⁴ diagonalization (Weisse et al., 2006). KPM expands spectral functions in Chebyshev
polynomials and evaluates them via recursive matrix–vector multiplications. Reconstructing
the moments of the Chebyshev expansion depends on the observable of interest and can
be computed through either a single inner product or through a trace, which is computed
using a stochastic trace (Skilling, 1988). Carefully chosen kernels (e.g., the Jackson) suppress
Gibbs oscillations and improve convergence of the truncated Chebyshev series. Because the
dominant cost is sparse matrix–vector products, KPM scales (nearly) linearly with the size of
the Hilbert space, which for non-interacting systems scales like the volume, and can be applied
to extremely large sparse Hamiltonians to compute quantities such as the density of states
(DOS) and DC conductivity (João & Lopes, 2019).

¹⁵ KPM.jl is a Julia implementation (Bezanson et al., 2017) of KPM for tight-binding models
in condensed matter physics, providing a high-performance, user-friendly toolbox. KPM.jl
¹⁶ targets large sparse Hamiltonians, integrates with CUDA.jl for automatic GPU acceleration
¹⁷ when available, and is designed for scalability and ease of integration into Julia-based workflows
¹⁸ for large-scale spectral and transport calculations.

²⁹ Statement of need

³⁰ KPM.jl provides a high-performance implementation of the Kernel Polynomial Method tailored
31 to tight-binding models. The method avoids ever doing a full diagonalization and instead
32 uses Chebyshev expansions, the package enables spectral and transport calculations on very
33 large sparse Hamiltonians that are infeasible with exact diagonalization (ED). It fills the gap
34 between low-level C/Fortran libraries and interactive, reproducible Julia workflows by offering:

- ³⁵ 1. **Scalability:** Capable of handling large sparse matrices representing realistic tight-binding
models.
- ³⁷ 2. **Versatility:** Support for DOS and LDOS, as well the DC conductivity (both longitudinal
and Hall) as well as linear and nonlinear optical response functions.
- ³⁹ 3. **Performance:** Automatic GPU acceleration via CUDA.jl when available.
- ⁴⁰ 4. **Integration:** As a Julia package, it easily interfaces with other tools in the Julia ecosystem
for Hamiltonian generation and data analysis.

42 In condensed matter physics, understanding the effects of disorder, interactions, and complex
 43 lattice geometries often requires numerical simulations of very large Hamiltonians. Traditional
 44 ED methods for computing the full spectrum are limited to relatively small system sizes
 45 (typically $N \sim 10^4$ states), which can be insufficient to resolve the spectral features of
 46 disordered systems or incommensurate structures like twisted bilayer graphene. KPM.jl is
 47 especially useful for studies of disorder, moiré systems, and topological materials where large
 48 system sizes ($N \sim 10^7$ states) are essential to capture realistic spectral and transport behavior.

49 Software design

50 KPM.jl is designed with modularity and performance in mind. The package operates on sparse
 51 Hamiltonians and computes Chebyshev moments using stochastic trace estimation with random
 52 vectors. The core functionality is divided into three main tiers corresponding to the complexity
 53 of the response function:

- 54 **Density of States (1D):** The KPM.kpm_1d function computes the Chebyshev moments
 55 for the DOS. It supports stochastic estimation using multiple random vectors (NR) and
 56 allows users to supply custom input vectors to compute the LDOS. The moments are
 57 converted to the spectral density $\rho(E)$ using KPM.dos.
- 58 **Linear Response (2D):** For transport properties like DC conductivity, KPM.kpm_2d
 59 calculates the moments required for the Kubo-Greenwood formula involving two current
 60 operators (J_x, J_y). The function KPM.d_dc_cond processes these moments to obtain the
 61 energy-dependent conductivity $\sigma_{\alpha\beta}(E)$ with $\alpha, \beta = x, y, z$.
- 62 **Nonlinear Response (3D):** The package includes specialized routines (KPM.kpm_3d) for
 63 frequency-dependent linear and nonlinear responses, such as the Circular Photogalvanic
 64 Effect (CPGE). This involves computing moments for three operators (J_x, J_y, J_z)
 65 and post-processing them (KPM.d_cpge) to extract the second-order conductivity
 66 $\chi_{xyz}(\omega_1, \omega_2)$.

67 The software automatically detects available hardware and offloads matrix-vector multiplications
 68 to a GPU if a compatible CUDA device is present (KPM.whichcore()), ensuring efficient
 69 performance on modern clusters. Further memory can be saved by computing the matrix
 70 elements of H and J on the fly, which is not implemented here.

71 Example Usage

72 The following minimal example computes the DOS of a 1-D tight-binding chain using KPM.jl.

```

using KPM
using LinearAlgebra
using SparseArrays
using Plots

# Simple dense 1D tight-binding Hamiltonian (periodic)
function tb1dchain(N::Integer; t::Real=1.0)
    H = zeros(Float64, N, N)
    for i in 1:(N-1)
        H[i, i+1] = -t
        H[i+1, i] = -t
    end
    H[1, N] = -t
    H[N, 1] = -t
    return H
end

```

```

# Parameters
N = 500          # system size
NC = 256         # Chebyshev order
NR = 32          # number of random vectors for stochastic trace
nE = 1000         # output energy grid points

H = tb1dchain(N)
# Rescale H -> (-1, 1)
Hsparse = sparse(H.*(@im)) # make the Hamiltonian sparse under complex number
b, H_norm = KPM.normalizeH(Hsparse)

# Compute Chebyshev moments (DOS)
mu = KPM.kpm_1d(H_norm, NC, NR)    # returns moments (array-like)

# Reconstruct DOS on a grid and map energies back to physical scale
E, rho = KPM.dos(mu, b; kernel = KPM.JacksonKernel, N_tilde=nE)

# Analytical DOS
rho_exact = zeros(length(E))
mask = abs.(E) .< 2
rho_exact[mask] = 1.0 ./ (pi * sqrt.(4 .- E[mask].^2))

# plot the DOS
plot(E, rho, xlabel="E", ylabel="DOS", label="KPM")
plot!(E, rho_exact, lw=1, ls=:dash, label="Analytic")

```

73 The final DOS is shown in Figure 1. Discrepancies between the KPM and analytic results
74 arise from the finite system size, the truncated KPM expansion order, and stochastic trace
75 estimation error.

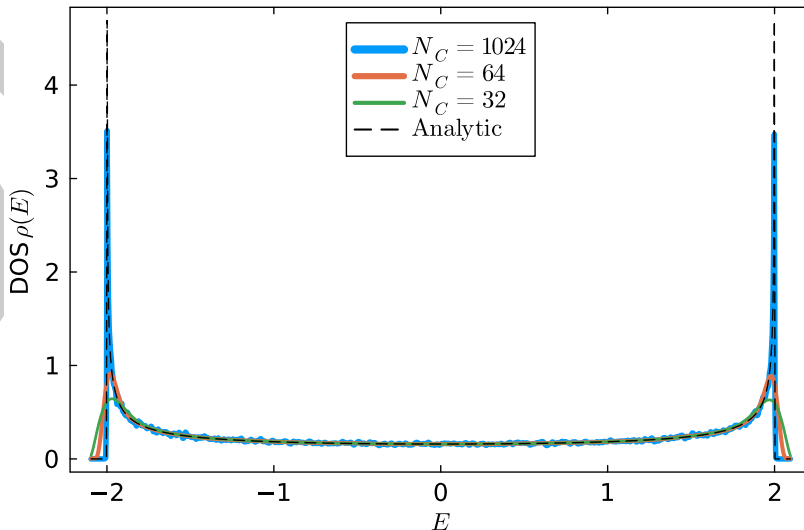


Figure 1: Density of states for a simple 1D tight-binding chain $L = 10^4$: KPM (solid) with various expansion order $N_C = 16, 32, 1024$ vs. analytic (dashed). The number of random vectors for the stochastic trace is $N_R = 10$.

76 Research impact statement

77 KPM.jl has been utilized in numerous studies to investigate electronic structure and response
78 in complex materials:

- 79 1. **Moiré systems and disorder:** Enabled large-scale simulations of twisted bilayer graphene
80 and demonstrated how twist-angle disorder broadens flat bands and modifies spectral
81 features (Chang et al., 2024; Chou et al., 2020; Fu et al., 2020; Wilson et al., 2020; Yi
82 et al., 2022).
- 83 2. **Experimentally relevant transport calculations:** Applied to transport modeling based on
84 tight-binding models derived from DFT+U to directly compare theory with experiment
85 (Liu et al., 2021; L. Wu et al., 2020; T.-C. Wu et al., 2025).
- 86 3. **Effects of Quasiperiodic potentials:** Used to compute conductivity and disorder-averaged
87 spectral properties and Green's function in disordered materials (Fu et al., 2021; Yi et
88 al., 2022).
- 89 4. **Nonlinear optical responses and disordered topological material:** Employed to calculate
90 nonlinear responses such as the CPGE in disordered topological semimetals and to
91 identify spectral signatures of surface and bulk phase transitions in disordered axion
92 insulators (Grindall et al., 2025; A.-K. Wu et al., 2024).
- 93 5. **Method benchmarking and numerical validation:** Served as a reference implementation for
94 comparing and validating new Chebyshev-regularization and spectral-density algorithms
95 (Yi et al., 2025).

96 These applications demonstrate the package's capability to tackle cutting-edge problems in
97 condensed matter theory.

98 AI usage disclosure

99 GitHub Copilot was used to assist with updating CUDA-related code, improving tests and
100 documentation, and polishing the manuscript for clarity and readability. The authors reviewed,
101 edited, and validated all AI-assisted contributions and take full responsibility for the content of
102 this publication.

103 Acknowledgements

104 We acknowledge the support of NSF Career Grant No. DMR-1941569, NSF Grant No. DMR-
105 2515945, US Department of Energy Office of Science, Basic Energy Sciences, under Award
106 No. DESC0026023 and the Alfred P. Sloan Foundation through a Sloan Research Fellowship.
107 J.H.W. acknowledges support from the National Science Foundation under Grant Number
108 DMR-2238895.

109 References

- 110 Bezanson, J., Edelman, A., Karpinski, S., & Shah, V. B. (2017). Julia: A fresh approach to
111 numerical computing. *SIAM Review*, 59(1), 65–98. <https://doi.org/10.1137/141000671>
- 112 Chang, Y., Yi, J., Wu, A.-K., Kugler, F. B., Andrei, E. Y., Vanderbilt, D., Kotliar, G., &
113 Pixley, J. H. (2024). Vacancy-induced tunable kondo effect in twisted bilayer graphene.
114 *Phys. Rev. Lett.*, 133, 126503. <https://doi.org/10.1103/PhysRevLett.133.126503>
- 115 Chou, Y.-Z., Fu, Y., Wilson, J. H., König, E. J., & Pixley, J. H. (2020). Magic-angle semimetals
116 with chiral symmetry. *Phys. Rev. B*, 101, 235121. <https://doi.org/10.1103/PhysRevB.101.235121>

- 118 Fu, Y., König, E. J., Wilson, J. H., Chou, Y.-Z., & Pixley, J. H. (2020). Magic-angle semimetals.
119 *Npj Quantum Materials*, 5(1), 71. <https://www.nature.com/articles/s41535-020-00271-9>
- 120 Fu, Y., Wilson, J. H., & Pixley, J. H. (2021). Flat topological bands and eigenstate criticality
121 in a quasiperiodic insulator. *Phys. Rev. B*, 104, L041106. <https://doi.org/10.1103/PhysRevB.104.L041106>
- 123 Grindall, C., Tyner, A. C., Wu, A.-K., Hughes, T. L., & Pixley, J. H. (2025). Separate surface
124 and bulk topological anderson localization transitions in disordered axion insulators. *Phys.*
125 *Rev. Lett.*, 135, 226601. <https://doi.org/10.1103/v7x8-ghfy>
- 126 João, S. M., & Lopes, J. M. V. P. (2019). Basis-independent spectral methods for non-linear
127 optical response in arbitrary tight-binding models. *J. Phys. Condens. Matter*, 32(12),
128 125901. <https://iopscience.iop.org/article/10.1088/1361-648X/ab59ec>
- 129 Liu, X., Fang, S., Fu, Y., Ge, W., Kareev, M., Kim, J.-W., Choi, Y., Karapetrova, E.,
130 Zhang, Q., Gu, L., Choi, E.-S., Wen, F., Wilson, J. H., Fabbris, G., Ryan, P. J., Freeland,
131 J. W., Haskel, D., Wu, W., Pixley, J. H., & Chakhalian, J. (2021). Magnetic weyl
132 semimetallic phase in thin films of $\text{Eu}_2\text{Ir}_2\text{O}_7$. *Phys. Rev. Lett.*, 127, 277204. <https://doi.org/10.1103/PhysRevLett.127.277204>
- 134 Skilling, J. (1988). The axioms of maximum entropy. In *Maximum-entropy and bayesian*
135 *methods in science and engineering: foundations* (pp. 173–187). Springer. https://link.springer.com/content/pdf/10.1007/978-94-009-3049-0_8.pdf=chapter+toc
- 137 Weisse, A., Wellein, G., Alvermann, A., & Fehske, H. (2006). The kernel polynomial method.
138 *Rev. Mod. Phys.*, 78, 275–306. <https://doi.org/10.1103/RevModPhys.78.275>
- 139 Wilson, J. H., Fu, Y., Das Sarma, S., & Pixley, J. H. (2020). Disorder in twisted bilayer graphene.
140 *Phys. Rev. Res.*, 2, 023325. <https://doi.org/10.1103/PhysRevResearch.2.023325>
- 141 Wu, A.-K., Guerci, D., Fu, Y., Wilson, J. H., & Pixley, J. H. (2024). Absence of quantization
142 in the circular photovoltaic effect in disordered chiral weyl semimetals. *Phys. Rev. B*,
143 110, 014201. <https://doi.org/10.1103/PhysRevB.110.014201>
- 144 Wu, L., Wen, F., Fu, Y., Wilson, J. H., Liu, X., Zhang, Y., Vasiukov, D. M., Kareev, M. S.,
145 Pixley, J. H., & Chakhalian, J. (2020). Berry phase manipulation in ultrathin SrRuO_3
146 films. *Phys. Rev. B*, 102, 220406. <https://doi.org/10.1103/PhysRevB.102.220406>
- 147 Wu, T.-C., Chang, Y., Wu, A.-K., Terilli, M., Wen, F., Kareev, M., Choi, E. S., Graf, D.,
148 Zhang, Q., Gu, L., & others. (2025). Electronic anisotropy and rotational symmetry
149 breaking at a weyl semimetal/spin ice interface. *Science Advances*, 11(24), eadr6202.
150 <https://www.science.org/doi/full/10.1126/sciadv.adr6202>
- 151 Yi, J., König, E. J., & Pixley, J. H. (2022). Low energy excitation spectrum of magic-angle
152 semimetals. *Phys. Rev. B*, 106, 195123. <https://doi.org/10.1103/PhysRevB.106.195123>
- 153 Yi, J., Massatt, D., Horning, A., Luskin, M., Pixley, J. H., & Kaye, J. (2025). *A high-order*
154 *regularized delta-chebyshev method for computing spectral densities*. <https://arxiv.org/abs/2512.03149>